Bioelectrochemistry 144 (2022) 108037

Contents lists available at ScienceDirect

Bioelectrochemistry

journal homepage: www.elsevier.com/locate/bioelechem

An electrochemical biosensor based on ARGET ATRP with DSN-assisted target recycling for sensitive detection of tobacco mosaic virus RNA

Yaping Zhang, Peipei Li, Mengyuan Hou, Luyao Chen, Jianfeng Wang *, Huaixia Yang *, Weisheng Feng *

Pharmacy College, Henan University of Chinese Medicine, Zhengzhou 450046, PR China

ARTICLE INFO

Article history:
Received 18 October 2021
Received in revised form 4 December 2021
Accepted 6 December 2021
Available online 8 December 2021

Keywords:
Tobacco mosaic virus
ARGET ATRP
DSN-assisted target recycling
Electrochemical biosensor

ABSTRACT

Herein, an electrochemical biosensor for detecting tobacco mosaic virus (TMV) RNA is constructed by activator regenerated by electron transfer atom transfer radical polymerization (ARGET ATRP) combined with duplex-specific nuclease (DSN)-assisted target recycling. First, the captured DNA (cDNA) is self-assembled on the electrode surface and hybridizes with the TMV RNA (tRNA) to form cDNA/tRNA hybrids. And then the initiator of ARGET ATRP (α-bromoisobutyric acid, BMP) is attached to the cDNA via an amide bond and later triggers ARGET ATRP. Many electroactive monomers (ferrocenylmethyl methacrylate, FMMA) are polymerized and a remarkable electrical signal response of ferrocene (Fc) is obtained. However, with the present of DSN, DSN cleaves the cDNA/tRNA hybrid and releases tRNA to hybridize with another cDNA, thereby causing significant shortening of the length of the cDNA. The number of polymer chains on the electrode surface is drastically reduced, which is followed by a noticeable reduction in the signal of Fc. The method shows high sensitivity, superior selectivity, excellent stability and good reproducibility under optimal conditions with the limit of detection (LOD) of 2.9 fM. Furthermore, the biosensor showed satisfactory applicability in detecting tRNA in real samples, thereby demonstrating the potential of the method for practical TMV RNA detection.

Contents

1. Introduction . . . 2
2. Experimental section . . . 2
 2.1. Chemicals and reagents . . . 2
 2.2. Apparatus . . . 2
 2.3. Preparation of MCH/cDNA-modified electrode . . . 2
 2.4. Detection of TMV RNA . . . 3
 2.5. Preparation of total RNA in healthy leaves of rehmannia . . . 3
3. Results and discussion . . . 3
 3.1. Principle of the TMV RNA electrochemical detection . . . 3
 3.2. Feasibility study . . . 4
 3.3. Characterization of the fabricated biosensor . . . 4
  3.3.1. Electrochemical characterization . . . 4
  3.3.2. AFM characterization . . . 5
  3.3.3. Static water contact angles characterization . . . 5
 3.4. Optimization . . . 5
 3.5. Analytical performance . . . 5
 3.6. Selectivity, reproducibility and stability ability . . . 6
 3.7. Determination of tRNA in real samples . . . 7
4. Conclusion . . . 7
 Declaration of Competing Interest . . . 7

* Corresponding authors.
E-mail addresses: 2816589787@qq.com (J. Wang), yhx998@hactcm.edu.cn (H. Yang), fwsh@hactcm.edu.cn (W. Feng).

https://doi.org/10.1016/j.bioelechem.2021.108037
1567-5394/

Acknowledgments . . . 7
Appendix A. Supplementary material . . . 7
References . . . 7

1. Introduction

Nucleic acid analysis techniques are becoming increasingly important in areas such as environmental science [1], biochemistry [2,3], food safety [4] and disease diagnosis [5,6]. Therefore, improving the selectivity and sensitivity of nucleic acid molecular detection methods has become one of the most popular research topics. To date, with technological advances, various nucleic acid detection strategies have been used, such as gene chips, polymerase chain reaction (PCR) [7], fluorescence [8,9], surface plasmon resonance [10], and electrochemistry [11-13]. Among them, electrochemical biosensors have received much attention for their advantages such as fast response time, easy operation, and low cost. However, conventional electrochemical strategies are mostly based on equiproportional target-to-signal hybridization ratios, which affects their sensitivity [14]. Therefore, developing electrochemical sensors that are highly sensitive to trace components in biological samples remains challenging.

To improve the sensitivity of biosensors, a variety of strategies for signal amplification have been explored, such as the use of nanomaterials, enzyme catalysis, and chain propagation of polymers [15]. Of these, enzyme-catalyzed reactions have attracted the attention of researchers due to their high reaction efficiency, inherent catalytic activity, and specificity. In recent years, duplex-specific nuclease (DSN)-assisted target has been recycling broadly used in RNA detection due to its high specificity and satisfactory selectivity [16-18]. In standard DSN-assisted target recycling, DSN can selectively cleave DNA from double-stranded DNA or DNA-RNA heterodimers. Nevertheless, DSN has no effect on single-stranded RNA, double-stranded RNA or single-stranded DNA and distinguishes well between perfectly matched and nonexactly matched short double genes [19,20]. Thus, in the presence of DSN, the target RNA is released and hybridized to another ssDNA, thereby causing amplification of the target cycle. Zhang et al. constructed a non-fixed electrochemical impedance biosensor by using DSN-assisted target recycling, which achieved highly sensitive detection of microRNA [21]. However, although DSN-assisted target recycling is simple and fast, this method based on single enzyme amplification is still not sensitive enough for ultra-microRNA detection. Therefore, improving the sensitivity of the assay by further amplification of the electrochemical signal is necessary.

Atomic transfer radical polymerization (ATRP), which was first proposed by Matyjaszewski and Wang in 1995, is a technique for live/controlled polymerization [22]. By establishing a dynamic balance between low concentrations of active species and high concentrations of dormant species, the reaction enables the successful synthesis of polymers with precise structure and function [14]. Thanks to its wide range of monomers, mild polymerization conditions, and ease of control, among other properties, ATRP has been widely used in the fields of surface functionalization [23], material synthesis [24], and biosensors [25,26]. Liu and her colleagues constructed a highly sensitive electrochemical DNA biosensor by using ATRP with a detection limit of 0.14 fM [27]. In conventional ATRP, metal catalysts at high concentrations (1000 to 10,000 ppm) are required to overcome irreversible radical termination and produce the required concentration of deactivator because of the continuous radical effect. Moreover, the demand for an oxygen-free environment restricts the broad application of this method [28,29]. Electron transfer activated regeneration ATRP (ARGET ATRP) was developed by Matyjaszewsk et al. by introducing a reducing agent [30]. It permits the reaction to take place at low concentration of copper catalyst and eliminates the need for an oxygen-free environment, which has potential benefits in terms of cost control and greening.

In this work, an electrochemical biosensor for sensitively detecting tobacco mosaic virus (TMV) RNA sensitively was constructed by ARGET ATRP in combination with DSN-assisted target recycling. TMV is a common plant virus that has caused severe losses to the world's agricultural economies since the end of the 19th century [31]. Apart from infecting common cash crops such as tobacco and peppers, it can also infect medicinal plants, including rehmannia and radix pesudostellariae, thereby affecting their yield and quality [32,33]. Thus, in this work, TMV RNA (tRNA) was selected as the target for detection. For this biosensor, hybridization of complementary nucleic acids ensured satisfactory specificity, and the intrinsic properties of dual signal amplification with ARGET ATRP and DSN-assisted target recycling guaranteed high sensitivity. This electrochemical biosensor demonstrated excellent analytical performance, high sensitivity, excellent specificity, good stability, and superior reproducibility and provides an electrochemical sensing platform with great potential for detecting TMV RNA.

2. Experimental section

2.1. Chemicals and reagents

Detailed information is provided in the supplementary material.

2.2. Apparatus

Detailed information is provided in the supplementary material.

2.3. Preparation of MCH/cDNA-modified electrode

Before being constructed, the gold electrode (GE) was polished the alumina of two grain sizes (0.3 μm and 0.05 μm) in turn, and cleaned ultrasonically using ethanol and ultrapure water. After that, the GE was soaked in a piranha solution that was freshly prepared from 98% H_2SO_4 and 30% H_2O_2 in a 3:1 vol ratio for 15 min and cleaned in the same way. Finally, the GE was electrochemically pretreated by immersing it in 0.5 M H_2SO_4 solution until overlapping cyclic voltammetry (CV) curves were acquired with potential range of 0.3–1.5 V.

First, the capture DNA (cDNA, 2 μM, 5 μL) was added to the GE and the cDNA/GE was maintained at room temperature overnight. Then, the cDNA/GE was then washed with a suitable amount of Tris-EDTA buffer solution (TE buffer, pH 7.4) to remove the nonspecific and loosely adsorbed cDNA. Afterward, the cDNA/GE was inserted into 300 μL 6-mercaptohexanol (MCH) at 37 °C for 30 min, so as to close the sites on the GE surface that were not

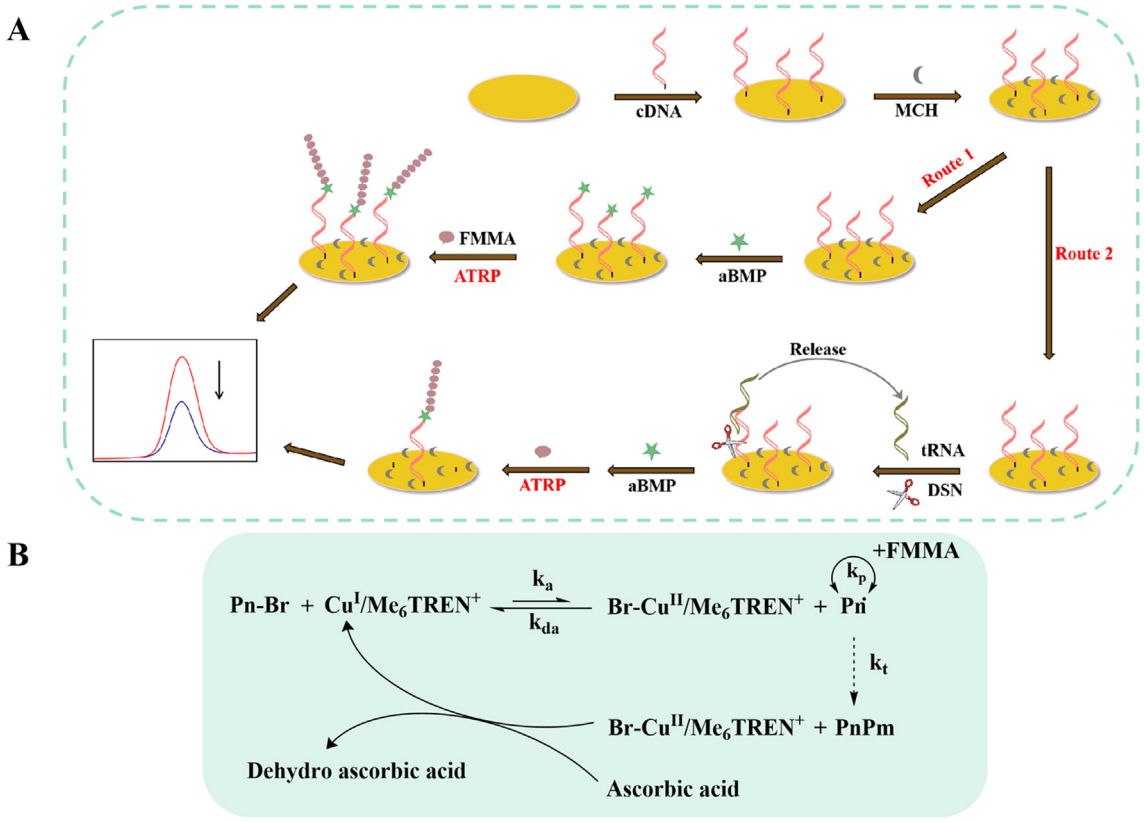

Scheme 1. (A) Schematic illustration of the prepared tRNA biosensor. (B) The mechanism of ARGET ATRP (Pn-Br = alkyl bromide, k_a = activation rate constant, k_{da} = deactivation rate constant, k_p = propagation rate constant, and k_t = termination rate constant).

occupied by cDNA and to prevent nonspecific adsorption of other materials. Following a moderate rinse with 70% ethanol and water, MCH/cDNA/GE was obtained.

2.4. Detection of TMV RNA

For the detection of tRNA, 10 μL of a mixed solution that contained a variable concentrations of tRNA and 2 U/mL DSN in 1 × DSN master buffer (50 mM Tris-HCl, 5 mM $MgCl_2$, 1 mM DL-dithiothreitol (DTT), pH 8.0) was added into the prepared MCH/cDNA/GE and incubated at 37 °C for 80 min. Following a moderate rinse with wash buffer, the electrode was dunked in 300 μL activated α-bromoisobutyric acid (aBMP) and reacted at 37 °C for 1 h. Afterward, the electrode surface was cleaned using DMSO and water in turn. Subsequently, the obtained GE was inserted into 200 μL of freshly prepared ARGET ATRP reaction solution and reacted at 37 °C for 1 h. Eventually, the prepared GE was immersed in Tris-HCl buffer (10 mM, pH 7.4) and measured using differential pulse voltammetry (DPV) by a traditional three-electrode system which was composed of a modified SE (2 mm in diameter), a saturated calomel electrode (SCE) and a platinum wire control electrode (initial potential: 0.00 V, final potential: 0.60 V, potential amplitude: 0.025 V, potential increase: 4 mV, and quiet time: 4 s).

2.5. Preparation of total RNA in healthy leaves of rehmannia

The extraction of total RNA from healthy rehmannia leaves was performed according to the technique that is described in Jin et al. with minor changes [34]. The steps are described in detail in the supplementary material.

3. Results and discussion

3.1. Principle of the TMV RNA electrochemical detection

The steps for the construction of an electrochemical sensor for the detection of tRNA based on ARGET ATRP and DSN-assisted target recycling are illustrated in Scheme 1A. Initially, cDNA and MCH were sequentially immobilized on the surface of the GE by self-assembly. This was done to build MCH/cDNA/GE via the self-assembly of Au-S bonds with the formation of RS-Au-SR complexes [19]. Next, for route 1, ARGET ATRP initiator BMP was tightly connected to the cDNA by forming an amide bond with the amino group at the 3′ end of the cDNA. Subsequently, using ferrocenylmethyl methacrylate (FMMA) as the monomer, a large number of electroactive probes were linked with BMP by the ARGET ATRP reaction, which were eventually able to produce a remarkable electrochemical signal. In route 2, when tRNA and DSN were titrated on MCH/cDNA/GE, tRNA was able to specifically recognize the oligonucleotide sequence of cDNA, thereby resulting in the formation of cDNA/tRNA. At the same time, the cDNA/tRNA hybrid was recognized and cleaved by the DSN, thus releasing tRNA. The released tRNA was able to bind to a large number of capture probes, which ultimately led to the cleavage of cDNA with the amino group at the 3′ end and significant DSN-assisted target recycling. As a result, BMP could not ligate to cDNA, and ARGET ATRP had difficulty occurring, which caused a dramatic reduction of the signal of ferrocene (Fc).

The mechanism of ARGET ATRP reaction is illustrated in Scheme 1B. The stable Br-Cu^{II}/Me_6TREN was reduced by reducing agent (acetic acid, AA) to catalytically active Cu^{I}/Me_6TREN, which could be homolytically cleaved with the initiator (P_n-Br) to produce deactivators (Br-Cu^{II}/Me_6TREN) and radicals ($P_n^{\blacksquare}$). The double

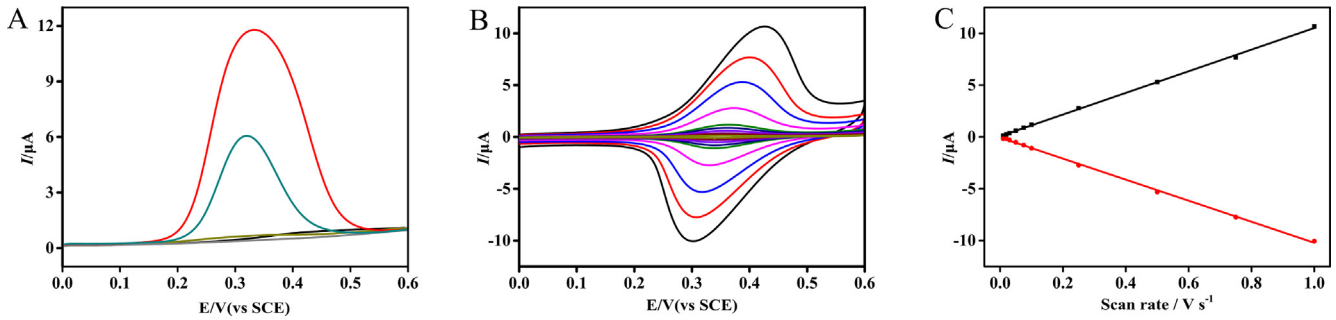

Fig. 1. (A) DPV curves of FMMA/BMP/MCH/GE (black line), FMMA/MCH/cDNA/GE (dark yellow line), BMP/MCH/cDNA/GE (gray line), FMMA/BMP/MCH/cDNA/GE (red line) and FMMA/BMP/MCH/cDNA/GE with tRNA and DSN (dark cyan line). (B) CV curves of FMMA/BMP/MCH/cDNA/GE at scan rates of 0.01–1 V s^{-1}. (C) The plots of the oxidation (marked black) and reduction (marked red) peak currents versus the scan rates in Fig. B.

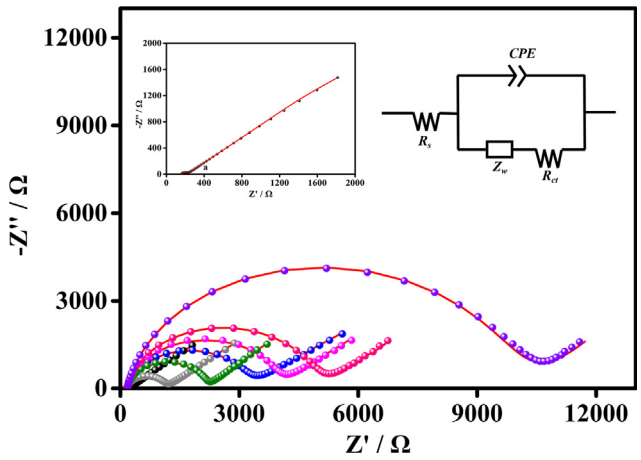

Fig. 2. Nyquist plots of GE (black sphere), cDNA/GE (gray sphere), MCH/cDNA/GE (blue sphere), MCH/cDNA/GE with tRNA (magenta sphere), MCH/cDNA/GE with tRNA and DSN (olive sphere), BMP/MCH/cDNA/GE (pink sphere) and FMMA/BMP/MCH/cDNA/GE (violet sphere). The inset was the equivalent circuit diagram of EIS. R_s was the solution resistance, *CPE* was the constant phase element, Z_w was the Warburg impedance, and R_{ct} was the charge transfer resistance, respectively.

bond addition of radicals ($P_n^{\blacksquare}$) to the monomer (FMMA) initiated polymerization, chain growth, and finally the formation of a polymer (P_nP_m). The coupling radical (P_nP_m) reacted with Br-Cu^{II}/Me_6-TREN to form a long polymeric chain (P_nP_m-X). Meanwhile, the simultaneous reduction of Br-Cu^{II}/Me_6TREN by excess AA to Cu^{I}/Me_6TREN could trigger a new round of polymerization. The ARGET ATRP reaction allowed for some reduction in the amount of metal catalyst, where the excess reducing agent permitted a small amount of oxygen to be present and did not affect the controlled polymerization of the reaction [30]. Significantly, the use of ARGET ATRP signal amplification and DSN-assisted target recycling significantly could be combined to improve the selectivity and sensitivity of the biosensor for TMV RNA detection.

3.2. Feasibility study

The current signals of electrodes fabricated by various approaches were measured using DPV to assess the feasibility of the proposed biosensor. It could be seen in Fig. 1A that no significant current signal was detected when any one of the cDNA (black line), BMP (dark yellow line) or FMMA (gray line) was missing. In contrast, for FMMA/BMP/MCH/cDNA (red line), a clear oxidation peak was observed at a potential of ~ 0.32 V, thereby indicating that BMP successfully triggered the polymerization chain reaction after linking to cDNA via amide bonds, and the final electrochemical signal was amplified. When tRNA and DSN were dropped simultaneously on the modified electrode, as shown by the dark cyan line of Fig. 1A, the DPV signal of Fc dropped significantly. Thus, the application of an electrochemical biosensor based on ARGET ATRP with DSN-assisted target recycling for sensitive detection of tRNA was feasible.

3.3. Characterization of the fabricated biosensor

3.3.1. Electrochemical characterization

The electrochemical properties of the FMMA/BMP/MCH/cDNA/GE surface were studied using CV. As shown in Fig. 1B, the redox peak of Fc was regularly strengthened as the scan rate was increased from 0.01 to 1 V s^{-1}. There was a clear linear relationship that existed between the redox current and the scan rate (Fig. 1C). Because the result was typical of surface-controlled redox processes, it was concluded that FMMA was successfully polymerized on the surface of electrode [27].

The surface properties of electrochemical biosensors based on ARGET-ATRP with DSN-assisted target recycling were characterized using electrochemical impedance spectroscopy (EIS), which is a key approach for characterizing the interfacial properties of modified electrodes. The nyquist diagram is fitted to an equivalent circuit model consisting of ohmic resistance (R_s), charge transfer resistance (R_{ct}), Warburg impedance (Z_w), and constant phase element (*CPE*) (Inset). The values of the equivalent circuit parameters of the fitting curves for the progressive production of the sensor were shown in Table S2. In the Nyquist plot, the semicircle of the impedance curve corresponds to the R_{ct} (the diameter of the semicircle) in the high frequency region [35]. Typical Nyquist plots of the impedance spectrum of the same electrode that were obtained step by step during successive preparations were shown in Fig. 2. Clearly, the bare GE showed a very small R_{ct} (~57.9 Ω, black sphere) prior to the self-immobilization of the cDNA, which was attributed to the rapid charge transfer kinetics. After successful modification of cDNA on the surface of the bare electrode, the R_{ct} rose to ~ 968.7 Ω (gray sphere), which was due to spatial barrier from cDNA monolayer. Similarly, the R_{ct} increased further (~3008 Ω, blue sphere) after MCH blocked the nonspecific binding site on the surface of GE in response to the formation of an MCH monomolecular layer that further impeded charge transfer. When tRNA was added, DNA/tRNA hybrid was formed and the R_{ct} value increased significantly (~3850 Ω, magenta sphere) due to electrostatic repulsion from the phosphorylation site of the RNA to $[Fe(CN)_6]^{3-/4-}$. Yet, when the DSN-assisted target recycling process occurred, the R_{ct} reduced to ~ 1973 Ω (olive sphere). This was because the cleaved of DNA/tRNA hybrid was broken up, the cDNA became shorter, and the released tRNA later bound to another cDNA to activate the next target recycling process. Eventually,

the potential resistance of the residual cDNA on the electrode was reduced markedly. In contrast, the introduction of BMP onto MCH/cDNA/GE reduced the hydrophilicity of the electrode surface and inhibited the access of redox probes to the electrode surface; thus, the modification of BMP further increased the R_{ct} (~4736 kΩ, pink sphere). Ultimately, after ARGET-ATRP, R_{ct} increased significantly (~9256 kΩ, violet sphere), which indicating the presence of a significant amount of electroactive polymer. As a result, the construction of the electrochemical biosensor for TMV RNA was realized successfully.

3.3.2. AFM characterization

The morphologies of different modified electrodes were characterized using AFM. The AFM results were shown in Fig. S1A–D. Fig. S1A showed that the height of the MCH/cDNA/GE was 10.0 nm. The height was 8.8 nm (Fig. S1B) when both tRNA and DSN were added to the MCH/cDNA/GE, which was lower than the height of MCH/cDNA/GE. The result confirmed the successful completion of the DSN-assisted target recycling process. After ARGET ATRP was triggered on the MCH/cDNA/GE, the height increased from 10.0 nm to 21.7 nm (Fig. S1C). However, the height increased to 15.7 nm after ARGET ATRP was triggered on the corrected electrode surface (Fig. S1D), which was lower than 21.7 nm. The above results provided further evidence that the detection of TMV RNA using an electrochemical biosensor based on AGRET ATRP and DSN-assisted target recovery was feasible.

3.3.3. Static water contact angles characterization

Finally, the hydrophilicity of progressively modified electrodes was explored with the use of static water contact angles (WCA). Fig. S2A showed a contact angle of 87.5° between the water and the bare electrode surface. After cDNA modification, the contact angle dropped to 74.3° (Fig. S2B) due to hydrophilicity in the cDNA. The contact angle further dropped to 68.8° (Fig. S2C) as the MCH was attached to the electrode, which could be attributed to the hydrophilic hydroxyl groups in the MCH. Furthermore, when tRNA was added to MCH/cDNA/GE, the contact angle continued to decrease (Fig. S2D). However, when DSN was present on the electrode, the contact angle instead increased to 71.5° (Fig. S2E). It demonstrated the success of DSN-assisted target recycling process, which meaning that the cDNA/tRNA hybrids were recognized by the DSN and the final cDNA was cleaved, thus releasing the tRNA. After immobilization of BMP to MCH/cDNA/GE via amide bonding, the hydrophilic contact angle decreased 59.8° (Fig. S2-F) because of amide bonding and halogen. Afterward, when FMMA was modified to BMP/MCH/cDNA/GE via ARGET ATRP, the contact angle of the electrode decreased from 59.8° to 53.2° (Fig. S2G). This was due to the hydrophilicity of the methacrylate. The above results were consistent with the results of AFM, indicating that the electrochemical biosensor was successfully constructed.

3.4. Optimization

The optimization of conditions is an important for obtaining the best possible analytical results. The electrochemical sensor relies on the dual amplification mechanism of DSN-assisted target recycling and the polymerization efficiency of the ATRP reaction. Therefore, the reaction time and amount of DSN are critical for DSN-assisted target recycling. Another important factor that affected the analytical performance of this biosensor is the reaction time of the ATRP.

First, using the current difference (ΔI) of the DPV peak of Fc as a signal, we optimized the reaction time and concentration of DSN. Here, the calculation of ΔI was based on the equation: $\Delta I = I - I_0$ (I_0 and I denote the DPV peak currents of FMMA/BMP/MCH/cDNA/GE without and with, respectively, the addition of tRNA and DSN. Fig. 3A showed that ΔI increased gradually as the DSN reaction time increased from 20 min to 80 min and reached a minimum at 80 min, after which there was no significant change. This might be the result of inactivation of the DSN and the cutting of the Fc-labeled substrate by the DSN over time [36]. Therefore, the reaction time of DSN was chosen to be 80 min. Next, from Fig. 3B it could be observed that ΔI continuously increased with increasing DSN concentration and then tended to stabilize after the concentration reached 2 U/mL. Therefore, 2 U/mL was identified as the optimal amount of DSN used in this method. Finally, the DPV peak current of Fc was studied in relation to the response time of ARGET ATRP. As shown in Fig. 2C, there was a gradual increase in signal as the reaction time increased, and the signal reached a peak at 60 min, after which it tended to stabilize. Consequently, 60 min was identified as the most suitable time for ARGET ATRP.

3.5. Analytical performance

The current response of the sensor was studied for a range of tRNA concentrations under optimized experimental conditions to explore the analytical performance of the electrochemical sensor. As shown in Fig. 4A, the peak current gradually decreased as the concentration of tRNA increased from 0.01 pM to 10 nM. namely, the values of ΔI rose as the concentration of tRNA increased. Moreover, a clear linear relationship was observed between ΔI and the logarithm of the tRNA concentrations (Fig. 4B). The following linear regression equation was obtained: ΔI (μA) = 1.4466 lg[C_{tRNA}/pM] + 4.0384 (R^2 = 0.998). Additionally, a limit of detection (LOD) of 2.9 fM (LOD = 3σ/slope) was obtained. As presented in Table 1, in comparison to several reported plant virus nucleic acid biosensors, our electrochemical biosensor had a relatively low

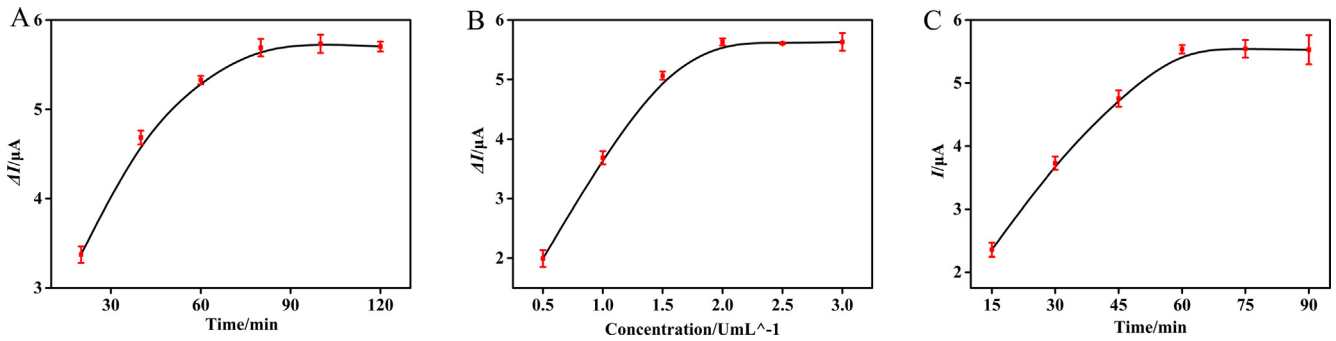

Fig. 3. Optimization of reaction parameters. The effects of (A) the reaction time and (B) the concentration of DSN, and (C) the ARGET ATRP reaction time on the proposed detection method for TMV RNA. The concentrations of tRNA used in the condition optimization were all 10 pM and error bars represented the standard deviation (n = 3).

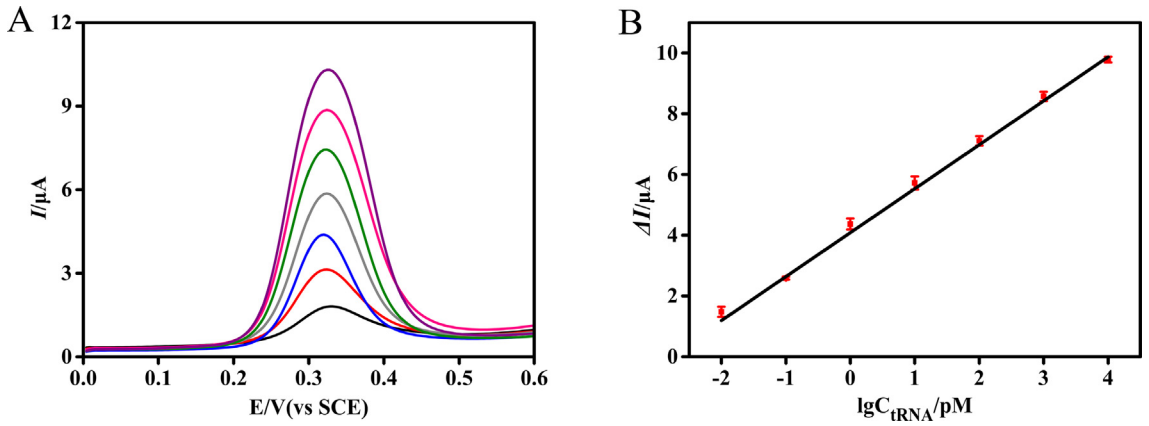

Fig. 4. (A) DPV responses to different concentrations of tRNA. The concentrations of tRNA were 10 fM (purple line), 0.1 pM (pink line), 1 pM (olive line), 10 pM (gray line), 0.1 nM (blue line), 1 nM (red line) and 10 nM (black line), respectively. (B) The linear relationship between ΔI and logarithm of the tRNA concentrations.

Table 1
Comparison of the constructed electrochemical biosensor with other developed biosensors.

Target	Texting method	Signal Amplification Strategy	L. R./M	LOD/M	Reference
Cucumber green mottle mosaic virus (CGMMV)	Ultraviolet	Terminal deoxynucleotidyl transferase coupled with DNAzymes amplification	1.0×10^{-13} - 2.0×10^{-9}	1.0×10^{-13}	[37]
Cauliflower mosaic virus 35 s (CaMV 35 s)	Fluorescence	backsplice junction combined with DSN-assisted target recycling	5.0×10^{-9} - 9.0×10^{-7}	2.0×10^{-9}	[38]
CaMV 35 s	Electrochemistry	SiO_2@CdTe quantum dots core–shell nanoparticles	1.0×10^{-13} - 5.0×10^{-10}	5.0×10^{-14}	[39]
CaMV 35 s	Electrochemstry	/	1.0×10^{-14} - 5.0×10^{-10}	6.0×10^{-14}	[40]
TMV RNA	Electrochemistry	ARGET ATRP combined with DSN-assisted target recycling	1.0×10^{-14} - 1.0×10^{-8}	2.9×10^{-15}	**This work**

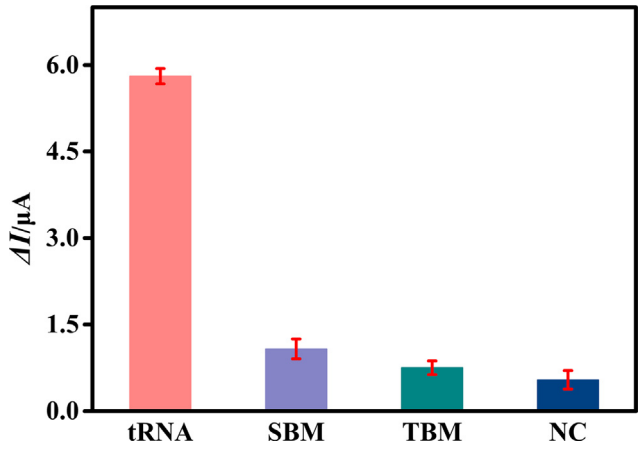

Fig. 5. Histogram of ΔI toward tRNA, SBM, TBM and NC. The concentrations of all RNAs were 10 pM.

detection limit due to the combination of ATRP signal amplification means with DSN-assisted target recycling.

3.6. Selectivity, reproducibility and stability ability

Initially, the current responses of 10 pM tRNA, single base mismatch RNA (SBM), triple base mismatch RNA (TBM) and non-complementary RNA (NC) were detected and compared under the same conditions to further investigate the selectivity of the biosensor. As could be seen from Fig. 5, the current responses of this sensor to SBM, TBM and NC changed slightly compared to that without the addition of tRNA. However, ΔI significantly increased with the addition of tRNA. In particular, the value of ΔI of tRNA was nearly 10 times higher than that of NC. This phenomenon might be due to the formation of DNA/RNA hybrids through base complementary pairing, which were then recognized by DSN, thereby resulting in DSN-assisted target recycling proceeding smoothly. Nevertheless, RNA that contained mismatched bases was unfavorable for forming DNA/RNA hybrids, which resulted in

Table 2
Recovery tests in real samples.

Sample	Added concentration/pM	Found concentration/pM	Recovery	RSD
1	0	–	–	3.253%
2	10	10.438	104.38%	2.938%
3	100	95.201	95.20%	2.030%
4	1000	964.206	96.42%	2.132%

difficult cleavage of cDNA by DSN. Afterward, the ARGET ATRP reaction proceeded well, resulting in small change in the electrochemical signal compared to tRNA.

Moreover, the reproducibility and stability of the strategy were evaluated. First, under the same experimental parameters, the reproducibility was assessed via intra- and inter-batch experiments (n = 5). For intra-batch analysis, the RSD of the ΔI value was 2.78%, and for inter-batch analysis it was 3.47%. Afterwards, a comparison of the response signal of the stored sensor with that of the newly prepared sensor was performed to evaluate the stability of the sensor. Even after two weeks of storage at −4 °C refrigerator, the ΔI of the stored electrode was approximately 91.88% (n = 3) of the signal of the freshly prepared electrode. The above results showed that the biosensor had desirable reproducibility and storage stability for the detection of tRNA.

3.7. Determination of tRNA in real samples

Recovery assays were performed on total RNA extracted from healthy rehmannia leaves in order to assess the performance of the biosensor in real samples. Apart from the 100-fold dilution, no other treatment was performed on the total RNA extract. The analytical results were displayed in Table 2. First, we examined the response signal of the sensor to the total RNA samples without tRNA addition. The experimental results showed that the response signal was basically no different from that of the experimental group without tRNA addition, with an RSD of 3.253%, which indicated that the biosensor had excellent interference immunity. Subsequently, 1000, 100 and 10 pM of tRNA was added to the total RNA extract, and the samples were assayed. The recoveries were ranged from 95.20% to 104.38%. Each sample was tested 3 times in parallel, and the RSDs were ranging from 2.030 to 2.938%. The experimental results strongly support the potential use of the proposed assay for the detection of TMV RNA in real samples.

4. Conclusion

A novel RNA biosensor was conveniently constructed using of ARGET ATRP and DNS-assisted target recycling. The sensitivity of the electrochemical biosensors could be ensured by using ARGET ATRP as a signal amplification strategy. In addition, the analytical performance and selectivity of the method were guaranteed by the DSN-assisted target recovery. The oxidation peak current of the biosensor exhibited good linearity with the concentration of the target RNA between 0.01 pM and 10 nM. In addition, it displayed ideal analytical properties such as low detection limits, and satisfactory selectivity, reproducibility and stability. Again, the biosensor performed satisfactorily in the analysis of target RNA in real samples, which demonstrated its potential for practical applications.

Declaration of Competing Interest

The authors declare that they have no known competing financial interests or personal relationships that could have appeared to influence the work reported in this paper.

Acknowledgments

This work was supported by Key Technology Research for the Characteristic Chinese Medicine Industry Chain of Rehmannia glutinosa (2017YFC1702800), the Major Science and Technology Projects in Henan Province (171100310500) and the project of the tackling of key scientific and technical problems in Henan Province (192102310033).

Appendix A. Supplementary material

Supplementary data to this article can be found online at https://doi.org/10.1016/j.bioelechem.2021.108037.

References

[1] W. Zhou, R. Saran, J. Liu, Metal Sensing by DNA, Chem. Rev. 117 (12) (2017) 8272–8325.
[2] H.M. Meng, H. Liu, H. Kuai, R. Peng, L. Mo, X.-B. Zhang, Aptamer-integrated DNA nanostructures for biosensing, bioimaging and cancer therapy, Chem. Soc. Rev. 45 (9) (2016) 2583–2602.
[3] O.L. Bodulev, I.Y. Sakharov, Isothermal nucleicacid amplification techniques and their use in bioanalysis, Biochem (Mosc). 85 (2) (2020) 147–166.
[4] B. Huo, Y. Hu, Z. Gao, G. Li, Recent advances on functional nucleic acid-based biosensors for detection of food contaminants, Talanta 222 (2021) 121565.
[5] S. Yadav, N.N. Sharma, J. Akhtar, Nucleic acid analysis on paper substrates (NAAPs): an innovative tool for Point of Care (POC) infectious disease diagnosis, Analyst 146 (11) (2021) 3422–3439.
[6] L.i. Liu, H. Lu, R. Shi, X.-X. Peng, Q. Xiang, B. Wang, Q.-Q. Wan, Y. Sun, F. Yang, G.-J. Zhang, Synergy of peptide-nucleic acid and spherical nucleic acid enabled quantitative and specific detection of tumor exosomal microRNA, Anal. Chem. 91 (20) (2019) 13198–13205.
[7] Z.Z. Hossain, J. Ferdous, S.M. Tulsiani, P.M. Jensen, A. Begum, Quantitative analysis of nucleic acid extraction methods for vibrio cholerae using real-time PCR and conventional PCR, Mymensingh, Med. J. 27 (2018) 327–335.
[8] C.Y. Lee, H. Kim, K.S. Park, H.G. Park, Nucleic acid-based fluorescent methods for the determination of DNA repair enzyme activities: A review, Anal. Chim. Acta 1060 (2019) 30–44.
[9] S. Lee, H. Jang, H.Y. Kim, H.G. Park, Three-way junction-induced isothermal amplification for nucleic acid detection, Biosens. Bioelectron. 147 (2020) 111762.
[10] H. Wu, S. Wang, S.F.Y. Li, Q.i. Bao, Q. Xu, A label-free lead(II) ion sensor based on surface plasmon resonance and DNAzyme-gold nanoparticle conjugates, Anal. Bioanal. Chem. 412 (27) (2020) 7525–7533.
[11] S. Takase, K. Miyagawa, H. Ikeda, Label-free detection of zeptomol miRNA via peptide nucleic acid hybridization using novel cyclic voltammetry method, Sensors (Basel). 20 (3) (2020) 836, https://doi.org/10.3390/s20030836.
[12] L. Hao, L. Zhao, G. Li, Y. Li, L. Ma, Y. Liu, W. Wang, J. Kong, Ultrasensitive detection of CYFRA 21–1 DNA via SI-RAFT based in-situ, Microchem J. 158 (2020) 105216.
[13] Z. Zhang, L. Huang, Z. Xu, P. Wang, Y. Lei, A. Liu, Efficient determination of PML/RARα fusion gene by the electrochemical DNA biosensor based on carbon dots/graphene oxide nanocomposites, Int. J. Nanomedicine 16 (2021) 3497–3508.
[14] L. Zhao, H. Yang, X. Zheng, J. Li, L. Jian, W. Feng, J. Kong, Dual signal amplification by polysaccharide and eATRP for ultrasensitive detection of CYFRA 21–1 DNA, Biosens. Bioelectron. 150 (2020) 111895.
[15] J. Li, L. Zhao, W. Wang, Y. Liu, H. Yang, J. Kong, F. Si, Polymer-functionalized carbon nanotubes prepared via ring-opening polymerization for electrochemical detection of carcinoembryonic antigen, Sens. Actuators B Chem. 328 (2021) 129031.
[16] J. Huang, J. Shangguan, Q. Guo, W. Ma, H. Wang, R. Jia, Z.i. Ye, X. He, K. Wang, Colorimetric and fluorescent dual-mode detection of microRNA based on duplex-specific nuclease assisted gold nanoparticle amplification, Analyst 144 (16) (2019) 4917–4924.
[17] A.D. Castañeda, N.J. Brenes, A. Kondajji, R.M. Crooks, Detection of microRNA by electrocatalytic amplification: A general approach for single-particle biosensing, J. Am. Chem. Soc. 139 (2017) 7657.
[18] F. Li, Y. Zhou, H. Yin, S. Ai, Recent advances on signal amplification strategies in photoelectrochemical sensing of microRNAs, Biosens. Bioelectron. 166 (2020) 112476.
[19] Q. Xiao, J. Li, X. Jin, Y. Liu, S. Huang, Ultrasensitive electrochemical microRNA-21 biosensor coupling with carboxylate-reduced graphene oxide-based signal-enhancing and duplexspecific nuclease-assisted target recycling, Sens. Actuators B Chem. 297 (2019) 126740.
[20] B. Li, X. Li, M. Wang, Z. Yang, H. Yin, S. Ai, Photoelectrochemical biosensor for highly sensitive detection of microRNA based on duplex-specific nuclease-triggered, J. Solid State Electrochem. 19 (2015) 1301–1309.
[21] J. Zhang, D.-Z. Wu, S.-X. Cai, M. Chen, Y.-K. Xia, F. Wu, J.-H. Chen, An immobilization-free electrochemical impedance biosensor based on duplex-specific nuclease assisted target recycling for amplified detection of microRNA, Biosens. Bioelectron. 75 (2016) 452–457.
[22] J. Wang, K. Matyjaszewski, Controlled/"Living" Radical Polymerization. Halogen Atom Transfer Radical Polymerization Promoted by a Cu(I)/Cu(II) Redox Process, J. Am. Chem. Soc. 117 (1995) 5614–5615.
[23] X. Jiang, M. Xi, L. Bai, W. Wang, L. Yang, H. Chen, Y. Niu, Y. Cui, H. Yang, D. Wei, Surface-initiated PET-ATRP and mussel-inspired chemistry for surface engineering of MWCNTs and application in self-healing nanocomposite hydrogels, Mater. Sci. Eng. C Mater. Biol. Appl. 109 (2020) 110553.
[24] A. Werner, V. Schmitt, G. Sèbe, V. Héroguez, Convenient synthesis of hybrid polymer materials by AGET-ATRP polymerization of pickering emulsions stabilized by cellulose nanocrystals grafted with reactive moieties, Biomacromolecules 20 (1) (2019) 490–501.

[25] H. Sun, Y. Qiu, Y. Lu, J. Kong, X. Zhang, Ultrasensitive DNA electrochemical biosensor based on MnTBAP biomimetic catalyzed AGET ATRP signal amplification reaction, Chem. Commun (Camb) 56 (49) (2020) 6636–6639.
[26] R. Bai, Y. Sun, M. Zhao, Z. Han, J. Zhang, Y. Sun, W. Dong, S. Li, Preparation of IgG imprinted polymers by metal-free visible-light-induced ATRP and its application in biosensor, Talanta 226 (2021) 122160.
[27] Q. Liu, L. Jian, R. Liu, H. Yang, J. Kong, X. Zhang, Metal-free photoinduced atom transfer radical polymerization for highly sensitive detection of lung cancer DNA, Chem. Eur. J. 26 (7) (2020) 1633–1639.
[28] P. Chmielarz, M. Fantin, S. Park, A.A. Isse, A. Gennaro, A.J.D. Magenau, A. Sobkowiak, K. Matyjaszewski, Electrochemically mediated atom transfer radical polymerization (eATRP), Prog. Polym. Sci. 69 (2017) 47–78.
[29] S. Hansson, V. Trouillet, T. Tischer, A.S. Goldmann, A. Carlmark, C. Barner-Kowollik, E. Malmström, Grafting efficiency of synthetic polymers onto biomaterials: a comparative study of grafting-from versus grafting-to, Biomacromolecules 14 (1) (2013) 64–74.
[30] W. Jakubowski, K. Min, K. Matyjaszewski, Activators regenerated by electron transfer for atom transfer radical polymerization of styrene, Macromolecules 9 (1) (2006) 39–45.
[31] J. Peng, K. Song, H. Zhu, W. Kong, F. Liu, T. Shen, Y. He, Fast detection of tobacco mosaic virus infected tobacco using laser-induced breakdown spectroscopy, Sci. Rep. 7 (2017) 44551.
[32] T.N. Erokhina, E.A. Lazareva, K.R. Richert-Pöggeler, E.V. Sheval, A.G. Solovyev, S. Y. Morozov, Subcellular localization and detection of tobacco mosaic virus ORF6 protein by immunoelectron microscopy, Biochem (Mosc) 82 (1) (2017) 60–66.
[33] M. Matsumoto, Y. Shoyama, I. Nishioka, H. Iwai, S. Wakimoto, Identification of viruses infected in Rehmannia glutinosa Libosch. var purpurea Makino and effect of virus infection on root yield and iridoid glycoside contents, Plant Cell Rep. 7 (1989) 636–638.
[34] P. Jin, Z. Zheng, H. Lu, J. Yan, G. Zheng, D. Wu, J. Lu, Roles of β-catenin, TCF-4, and survivin in nasopharyngeal carcinoma: correlation with clinicopathological features and prognostic significance, Cancer Cell Int. 19 (2019) 48.
[35] M.E. Strong, J.R. Richards, M. Torres, C.M. Becke, J.T.L. Belle, Faradaic electrochemical impedance spectroscopy for enhanced analyte detection in diagnostics, Biosens. Bioelectron. 177 (2021) 112949.
[36] J. Jiao, C. Li, L. Ning, L. Shi, L. Wang, Y. Xiang, G. Lia, Electrochemical detection of circRNAs based on the combination of backsplice junction and duplex-specific nuclease, Sens Actuators B Chem. 302 (2020) 127166.
[37] Y. Wang, J. Liu, H. Zhou, Visual Detection of Cucumber Green Mottle Mosaic Virus Based on Terminal Deoxynucleotidyl Transferase Coupled with DNAzymes Amplification, Sensors 19 (2019) 1298.
[38] B. Qiu, Y.-S. zhang, Y.-B. Lin, Y.-J. Lu, Z.-y. Lin, K.-Y. Wong, G.-N. Chen, A novel fluorescent biosensor for detection of target DNA fragment from the transgene cauliflower mosaic virus 35S promoter, Biosens. Bioelectron. 41 (2013) 168–171.
[39] Y. Li, L.i. Sun, Q. Liu, E.n. Han, N. Hao, L. Zhang, S. Wang, J. Cai, K. Wang, Photoelectrochemical CaMV35S biosensor for discriminating transgenic from non-transgenic soybean based on SiO_2@CdTe quantum dots core-shell nanoparticles as signal indicators, Talanta 161 (2016) 211–218.
[40] F. Zhan, X. Liao, F. Gao, W. Qiu, Q. Wang, Electroactive crown ester-Cu^{2+} complex with in-situ modification at molecular beacon probe serving as a facile electrochemical DNA biosensor for the detection of CaMV 35s, Biosens. Bioelectron. 92 (2017) 589–595.